

## EVOLUTION OF SULFUR GASES DURING COAL PYROLYSIS

M. S. Oh, A. K. Burnham, and R. W. Crawford

Lawrence Livermore National Laboratory, Livermore, CA, 94550

### 1. Introduction

The yields and rates of evolution of sulfur gases depend not only on pyrolysis conditions but also on the coal itself (1). The organic/inorganic forms of sulfur, as well as the secondary reactions of sulfur gases with solids and with other pyrolysis-generated gases, play an important role. Monitoring the time- and temperature-dependent evolution of sulfur-containing gases provides insight into the sulfur chemistry affecting evolution profiles (1,2). Programmed-temperature studies of sulfur gas evolution often have been limited to  $H_2S$ . In some cases, all sulfur gases have been studied collectively by reducing or oxidizing them to  $H_2S$  or  $SO_2$  (3,4). Recently, Calkins (5) studied the evolution of individual sulfur species from a Pyroprobe using Gas Chromatograph/Mass Spectrometer (GC/MS) and from isothermal flash pyrolysis. Boudou et al. (6) also identified some individual sulfur gases from isothermal pyrolysis using a Curie-point reactor in combination with MS, GC, and GC/MS.

In this study, we monitored the real-time evolution of sulfur gases during slow-heating pyrolysis via a triple quadrupole mass spectrometer (TQMS). We also monitored the evolution of hydrocarbon gases, water, and carbon oxides. We compared the evolution profiles of sulfur gases and related them to the rank of the coal, the organic and inorganic sources of sulfur in each coal sample, and the evolution of other pyrolysis-generated gases. We also studied the extent of secondary reactions by varying the pyrolysis conditions.

### 2. Experimental

A schematic of the experimental set-up is shown in Fig. 1. Coal was pyrolyzed in a 1.5-cm-i.d. quartz tube, placed in a 1.9-cm-i.d. three-zone furnace. The control thermocouples for the top and bottom zones were embedded in the furnace wall, while the thermocouple for the mid-zone was placed between the furnace wall and the reactor. Another thermocouple was inserted into the center of the coal-sand bed, and the average bed temperature was calculated from the wall and the center temperatures. Coal particles were diluted with quartz sand to prevent the bed from being plugged because of softening and agglomeration of coal. Coal was then heated from 25°C to 900°C at a heating rate of 4.5°C/min.

To examine the effect of secondary reactions on the observed products, we varied the amount of coal from 0.5 to 2.5 g and the argon flow rate from 34 to 169 cc/min. Compared to our reference conditions of 0.5 g and 34 cc/min, the experiment with sample size of 2.5 g and 34 cc/min argon flow represents a five-fold increase in pyrolysis gas partial pressure at nearly constant gaseous residence time. For the experiment in which both the sample size and argon flow were increased, gaseous partial pressures remained constant, but the gaseous residence time decreased.

To monitor the evolution of water and naphtha, including thiophenes, we heated all the parts, from the pyrolyzer to the TQMS. A constant flow of argon swept volatiles to a glass wool trap that was placed in an oven at -130°C to condense high boiling liquid products (tar). All transport lines from the trap to the TQMS were maintained at  $T > 140^\circ\text{C}$ .

In the TQMS operation, both normal mass scans (ms mode) and daughter ion scans (ms/ms mode) were used in all experiments. Details of the TQMS and the ms and ms/ms mode operation were described elsewhere (7). Table 1 summarizes the parent/daughter pairs for sulfur gases we monitored. All gases in Table 1, except  $\text{H}_2\text{S}$  and  $\text{SO}_2$ , are calibrated using analyzed commercial standards with the concentration levels about 200 ppm. We used a 981-ppm standard for  $\text{H}_2\text{S}$ , and  $\text{SO}_2$  was not calibrated.

We chose eight Argonne premium coal samples for our work because of their diverse properties, high quality, and wide-spread use by other researchers. Among the eight coals, we studied in detail two coals with the highest and the lowest sulfur contents. Illinois No. 6 high volatile bituminous coal (ILHVB) had the highest sulfur content (5.4%), while Blind Canyon Seam high volatile bituminous coal (BCHVB) had the lowest (0.5%). The properties of these two coals, provided by Argonne National Laboratory or obtained from literature (8), are shown in Table 2. Samples were stored under nitrogen and we saw no aging effects. Sulfur gases from other coals are discussed qualitatively based on the data obtained from pyrolysis in a stainless steel reactor. In those experiments with the stainless-steel reactor, the main goal was to study hydrocarbon gases under well-defined temperatures.

### 3. Results

The TQMS has the sensitivity, selectivity, and speed to monitor the real-time evolution of individual species in a complex pyrolysis gas mixture. We monitored  $\text{H}_2\text{S}$  and  $\text{CH}_3\text{SH}$  in both ms and ms/ms modes, while other sulfur gases were monitored only in ms/ms mode which was necessary to differentiate them from hydrocarbon gases of the same molecular mass. For  $\text{H}_2\text{S}$  and  $\text{CH}_3\text{SH}$ ,  $m/z = 34$  and 48 in ms mode are free of hydrocarbon interferences because  $m/z = 34$  and 48 are rare fragments of hydrocarbons. However,  $m/z = 48$  has to be corrected for  $\text{SO}_2$  fragments when  $\text{SO}_2$  is abundant.

For all eight coals, there are three temperature regions at which sulfur gases evolve under the given time-temperature history. Although the exact temperature of the maximum rate of evolution ( $T_{\text{max}}$ ) varies with the coal, the three regions are roughly  $< 200^\circ\text{C}$ ,  $400^\circ\text{C}$ - $500^\circ\text{C}$ , and  $500^\circ\text{C}$ - $600^\circ\text{C}$ .

At temperatures lower than  $200^\circ\text{C}$ , the only sulfur gas observed was  $\text{SO}_2$ . Low temperature evolution implies the existence of loosely bound, trapped, or adsorbed  $\text{SO}_2$ . However,  $\text{SO}_2$  evolution seems to be very sensitive to pyrolysis conditions. More low-temperature  $\text{SO}_2$  was detected as the ratio of coal to sweep-gas flow rate was increased. Experiments with a 316-stainless-steel reactor showed no  $\text{SO}_2$  at this temperature region, suggesting a reaction of  $\text{SO}_2$  with the stainless steel.

Figure 2 shows evolution profiles of eight other sulfur gases between  $200$  and  $800^\circ\text{C}$  from two coals, ILHVB (solid lines) and BCHVB (dotted lines). Because of the low sulfur content of BCHVB, only four major sulfur gases were detected. Most of the organic pyrolysis reactions occur between  $350$  and  $500^\circ\text{C}$ . While all gases have a peak in this temperature region,  $\text{H}_2\text{S}$ ,  $\text{COS}$ , and  $\text{CS}_2$  have a second peak between  $550$  and  $600^\circ\text{C}$ . While the high temperature source is clearly pyrite decomposition, the lower temperature source is more complicated.

Figure 3 compares the evolution profile of four organic sulfur compounds with the corresponding hydrocarbons. The sulfur compound precedes its corresponding hydrocarbon in all cases. While  $T_{\text{max}}$  for  $\text{CH}_4$  is substantially higher than those for other hydrocarbons, methanethiol is evolved at approximately the same temperature as the other thiols.

The evolution profiles in Fig. 2 are similar to those reported previously for Green River shale. Burnham et al. (2) noted that most of the  $\text{H}_2\text{S}$  evolved in the  $550^\circ\text{C}$  region could be shifted to the  $400$ - $450^\circ\text{C}$  range if pyrolysis occurs under self-

purging conditions (no auxiliary gas sweep). To explore this effect and other secondary reactions, we conducted two additional experiments on ILHVB coal. Table 3 compares the amounts of sulfur gases evolved under our standard conditions to those evolved from experiments representing higher product partial pressure ( $P_{vol}$ ) at similar residence time and shorter gaseous residence time ( $t_{res}$ ). The amounts of  $H_2S$  formed in the two temperature regions show no clear changes with these variations in conditions. The only observable effects are increased COS generation in the 550°C range at shorter  $t_{res}$  and changes in the amounts of  $CS_2$ .

In Fig. 4, we report  $T_{max}$  for  $H_2S$  and hydrocarbons from the experiments with a stainless-steel reactor. Even though some aspects of the sulfur-gas profiles were affected by reactions with the steel, Fig. 4 shows that  $T_{max}$  for  $H_2S$  depends on coal rank. The increase in  $T_{max}$  of the low temperature peak with the rank is greater than a similar increase in  $T_{max}$  for total organic volatiles (total ion current minus Ar,  $CO_2$ , CO,  $H_2O$ , and  $H_2S$ ).  $T_{max}$  for the high temperature  $H_2S$  peak shows more scatter, so the trend is not as clearly present as the low temperature  $H_2S$  peak. However, Whelen et al. (9) also observed an increase in  $T_{max}$  of both COS peaks with maturity in Type III kerogens, which suggests that our high temperature trend is real.

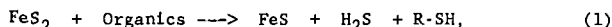
#### 4. Discussion

An obvious goal is to be able to relate the amounts and kinds of various sulfur components to the sulfur composition of the original coal and the processing conditions. The results in this paper provide only a small fraction of the information needed to achieve that goal. However, we have made significant progress.

The sulfur evolution profiles at temperatures between 400 and 500°C are a poorly defined combination of organic pyrolysis reactions and pyrite reactions. The source of sulfur can be both sulfur in the organic matrix as well as pyritic sulfur. Coal-matrix sulfur, especially in high volatile bituminous coals, exists as sulfides and thiophenes (4,5). Thus, sulfides and thiophenes are probably primary products of pyrolysis or products of tar cracking. Thiophenes are very stable at  $T < 500^\circ C$ , so they are not likely to go through gas phase secondary reactions. Hydrocarbon gases such as acetylene are also known to react with pyrite to form thiophenes (1). However, we found that, for Green River shale, removal of pyrite by acid treatment (7) and doping low-sulfur shales with pyrite (10) had negligible effects on the amount of thiophenes generated.

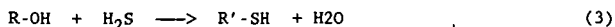
In contrast,  $H_2S$  and thiols can be generated by pyrite reactions. Pyrite decomposition is a strong function of grain size, gas environments, and pyrolysis conditions (2,11). Although the  $H_2S$  evolved below 500°C from well-swept fine particles can be attributed to organic sulfur (7), it can be shown from other data (2,7,12) that about two-thirds of the  $H_2S$  evolved below 500°C from Green River shale under self-purging conditions comes from pyrite. Unfortunately, we did not see any clear effect of pyrolysis conditions on  $H_2S$  formation reactions in ILHVB, as shown in Table 3. Apparently our range of conditions was too small to see the marked differences between gas sweep and self-purging conditions observed previously for Green River shale (2,13). We are also investigating other explanations for our observation, such as the effect of pyrite grain size and crystal structure.

Attar (1) indicated that organic matter can react with pyrite at temperatures as low as 250°C. The important reactions can be summarized in Reaction 1.



As implied in Reaction 1, the major source of hydrogen in  $H_2S$  formation reaction at these temperatures is probably hydrocarbons and hydrocarbon radicals both in

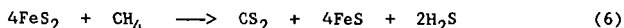
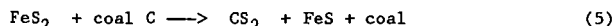
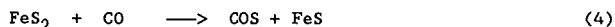
condensed and gas phases.  $\text{H}_2\text{S}$  and thiols are also likely to be involved in secondary reactions. For example,



For thiols, the gas phase secondary reactions may dominate, because the rate of evolution maximizes when  $\text{H}_2\text{S}$  evolution maximizes.

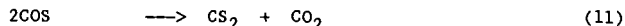
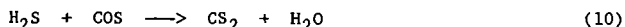
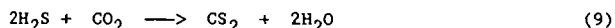
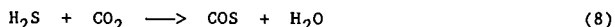
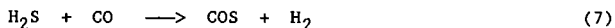
The results in Figure 2 show that only a few of the sulfur-containing compounds ( $\text{H}_2\text{S}$ , COS and  $\text{CS}_2$ ) are related to high-temperature pyrite reactions. Near  $600^\circ\text{C}$ , the evolution of hydrocarbon gases from pyrolysis, except  $\text{CH}_4$ , is essentially completed. Other pyrolysis gases available at this temperature are CO,  $\text{CO}_2$ ,  $\text{H}_2\text{O}$ , and  $\text{H}_2$ , of which the amounts are affected by char gasification, mineral dehydration, water-gas shift reaction, and carbonate mineral decomposition where possible. For the coal with high pyritic sulfur such as ILHVB, sulfur gases at this temperature are mainly from pyrite decomposition. Pyrite decomposes rapidly at temperatures above  $550^\circ\text{C}$ , and  $\text{H}_2\text{S}$  is the major product of pyrite decomposition. In our experiments, the source of hydrogen is probably  $\text{H}_2$ ,  $\text{H}_2\text{O}$ , and hydrogen in char; but the relative importance of each hydrogen donor is not yet clear.

Reactions to form COS and  $\text{CS}_2$  can be both gas-solid and gas phase secondary reactions. The pyrite reactions are:



In his review, Attar (1) claimed Reactions 4 and 5 are slow at  $T < 800^\circ\text{C}$ . However, Taylor et al. (14) found that the rate of formation of COS from the reaction of pyrite and 1% CO in argon was significantly fast even at  $500^\circ\text{C}$ . Calkins (5) suggested Reaction 6 takes place at  $T > 800^\circ\text{C}$ , so it may also be slow at the temperatures of interest here.

Examples (15) of the possible gas phase reactions at this temperature are:



Reaction 10 is known to occur at temperatures between  $350$  and  $900^\circ\text{C}$ , and Reaction 11 is slow but reaches a maximum at  $600^\circ\text{C}$  (16). Calkins's (5) observation of  $\text{CS}_2$  formation at  $T > 850^\circ\text{C}$  at the expense of  $\text{H}_2\text{S}$  indicates that Reactions 9 and 10 are possible. Our observation of the decrease in  $\text{CS}_2$  and the increase in COS yields at  $550^\circ\text{C}$  as  $t_{\text{res}}$  decreases supports Reactions 10 and 11. This observation also agrees with our previous results for Green River shale which found greater yields of COS from vacuum pyrolysis than in a self-purging reactor (7). Some of the sulfur from pyrite decomposition may also be trapped in the organic matrix (17).

We didn't detect elemental sulfur ( $\text{S}_2$  and  $\text{S}_8$ ), nor did Boudou et al. (5) find elemental sulfur from isothermal pyrolysis of non-oxidized coal. In our study, the

parent/daughter pair of 64/32, which could either be SO<sub>2</sub> or S<sub>2</sub>, had a very weak signal.

Because the evolution of sulfur gases always precedes that of hydrocarbon gases, organic sulfur components in coal, in general, seem to be more readily released during pyrolysis than non-heteroatom hydrocarbons. Lester et al. (18) made the same observation in their study with model compounds, although they found sulfur compounds and hydrocarbons evolve nearly simultaneously from coal in a chemical shock tube in which the coal residence time was 1.2-1.5 ms. We also find that T<sub>max</sub> for H<sub>2</sub>S and hydrocarbons both increase with the rank. The same trend is also seen for thiols and thiophenes. The increase in T<sub>max</sub> for hydrocarbons with rank reflects coal becoming more carbonaceous with rank.

#### 4. Conclusion

We studied the evolution of individual sulfur species during coal pyrolysis. Sulfur dioxide is the only sulfur gas that evolves at T < 200 °C, and all organic sulfur gases as well as COS, CS<sub>2</sub>, and H<sub>2</sub>S are found at 400-500°C, the temperature range of pyrolysis. The decomposition of pyrite at ~550°C produces H<sub>2</sub>S, COS, and CS<sub>2</sub>. Both gas-solid reactions and gas-phase secondary reactions are responsible for sulfur gas formation. The evolution of sulfur gases precedes that of hydrocarbon gases.

#### References

- (1) Attar, A. Fuel 1978, 57, 201-212.
- (2) Burnham, A. K.; Bey, N. K.; Koskinas, G. J. Oil Shale, Tar Sands, and Related Materials, ACS Symposium Series, 163, 1981, 61-77.
- (3) Attar, A.; Dupuis, F. Prepr. Pap.-Am. Chem. Soc., Div. Fuel Chem. 1978, 23(2), 44-53.
- (4) La count, R. B.; Anderson, R. R.; Friedman, S.; Blaustein, B.D. Prepr. Pap.-Am. Chem. Soc., Div. Fuel Chem. 1986, 31(1), 70-78.
- (5) Calkins, W. H. Energy & Fuels 1987, 1, 59-64.
- (6) Boudou, J. P.; Boulegue, J.; Malechaux, L.; Nip, M.; De Leeuw, J. W.; Boon, J. J. Fuel 1987, 66, 1558-1569.
- (7) Wong, C. M.; Crawford, R. W.; Burnham, A. K. Anal. Chem. 1984, 56(3), 390-395.
- (8) Wert, C. A.; Tseng, B. H.; Hsieh, K. C.; Ge, Y. P. Prepr. Pap.-Am. Chem. Soc., Div. Fuel Chem. 1987, 32(3), 250-259.
- (9) Whelan, J. K.; Solomon, P. R.; Deshpande, G. V.; Carangelo, R. M. Energy & Fuels 1988, 2, 65-73.
- (10) Fadeff, S. K.; Burnham, A. K.; Richardson, J. H. Organic and Pyritic Sulfur Determination in Oil Shale 1983, Lawrence Livermore National Laboratory, Livermore, CA, UCID-19751.
- (11) Maa, P. S.; Lewis, C. R.; Hamrin, C. E. Jr. Fuel 1975, 54, 62-69.
- (12) Singleton, M. F.; Koskinas, G. J.; Burnham, A. K.; Raley, J. H. Assay Products from Green River Oil Shale 1986, Lawrence Livermore National Laboratory, Livermore, CA, UCRL-53273 Rev. 1.
- (13) Wong, C. M.; Crawford, R. W.; Burnham, A. K. Prepr. Pap.-Am. Chem. Soc., Div. Fuel Chem. 1984, 29(3), 317-321.
- (14) Taylor, R. W.; Morris, C. J.; Crawford, R. W.; Miller, P. E. Internal Report, 1985, Lawrence Livermore National Laboratory, Livermore, CA.
- (15) Gmelin Handbuch der Anorganischen Chemie, 8th Ed., System No. 14, Part D 5, 1977, Springer-Verlag, Berlin, Heidelberg, 4.
- (16) Ferm, R. J. Chem. Rev. 1957, 57, 621-640.
- (17) Cleyle, P. J.; Caley, W. F.; Stewart, I.; Whiteway, S. G. Fuel 1984, 63, 1579-1582.
- (18) Lester, T. W.; Polavarapu, J.; Merklin, J. F. Fuel 1982, 61, 493-498.

Table 1. Parent/Daughter Mass Combination Employed in Sulfur Gas Identification.

Sulfur Species		Parent/Daughter Mass
H <sub>2</sub> S	Hydrogen Sulfide	34/32 or 34
CH <sub>3</sub> SH	Methanethiol	48/45 or 48
CO <sub>2</sub> S	Carbonylsulfide	60/32
C <sub>2</sub> H <sub>5</sub> SH	Ethanethiol	62/29
(CH <sub>3</sub> ) <sub>2</sub> S	Dimethylsulfide	62/47
SO <sub>2</sub>	Sulfur Dioxide	64/48
CS <sub>2</sub>	Carbon Disulfide	76/32
C <sub>3</sub> H <sub>7</sub> SH	Propanethiol	76/42
C <sub>4</sub> H <sub>4</sub> S	Thiophene	84/45
CH <sub>3</sub> C <sub>4</sub> H <sub>4</sub> S	Methylthiophene	97/53

Table 2. Elemental Analysis and Sulfur Forms (MAF basis) of Illinois No.6 Seam High Volatile Bituminous Coal (ILHVB) and Blind Canyon Seam High Volatile Bituminous Coal (BCHVB).

	ILHVB	BCHVB
% C	77.7	77.9
% H	5.7	6.0
% N	1.4	1.4
% O <sup>a</sup>	9.8	14.2
% Total S	5.4	0.5
Sulfur Forms:		
% Org. S	2.4	0.38 <sup>b</sup>
% Pyrite	3.0	N.A.
% Sulfate	0.01	N.A.

a. By difference.

b. Ref. 8.

#### Acknowledgments

We gratefully acknowledge Ken Foster's contribution to pyrolysis experiments, Armando Alcaraz's contribution to operation of TQMS, and Robert W. Taylor and Thomas T. Coburn for helpful discussion and reading the manuscript. This work was performed under the auspices of the U.S. Department of Energy by the Lawrence Livermore National Laboratory under Contract No. W-7450-Eng-48.

Table 3. Yields (STP cc/g coal) of Sulfur Gases under Different Pyrolysis Conditions.

Sweep Gas Flow Rate (cc/m):		34	34	169
Coal Sample Size (g):		0.52	2.54	2.58
Sulfur Species		Std. Run	High P <sub>vol</sub>	Shorter t <sub>res</sub>
H <sub>2</sub> S	1st Peak	4.800	6.161	5.503
	2nd Peak	8.230	8.702	9.113
	Total	13.030	14.863	14.616
COS	1st Peak	0.057	0.071	0.067
	2nd Peak	0.110	0.138	0.254
	Total	0.167	0.209	0.321
CS <sub>2</sub>	1st Peak	0.017	0.019	0.002
	2nd Peak	0.087	0.040	0.036
	Total	0.104	0.059	0.038
CH <sub>3</sub> SH		0.202	0.221	0.184
C <sub>2</sub> H <sub>5</sub> SH		0.031	0.036	0.029
(CH <sub>3</sub> ) <sub>2</sub> S		0.006	0.006	0.005
C <sub>3</sub> H <sub>7</sub> SH		0.007	0.009	no data
C <sub>4</sub> H <sub>9</sub> S		0.022	0.020	0.023
CH <sub>3</sub> C <sub>4</sub> H <sub>4</sub> S		0.076	0.072	0.089

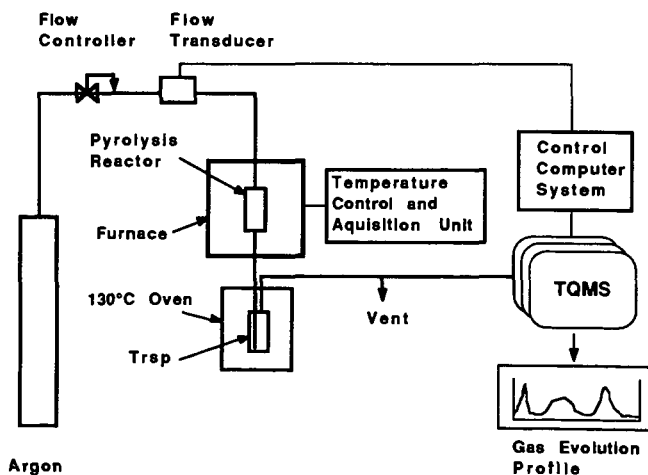


Fig. 1. Schematic of experimental set-up for gas evolution studies.

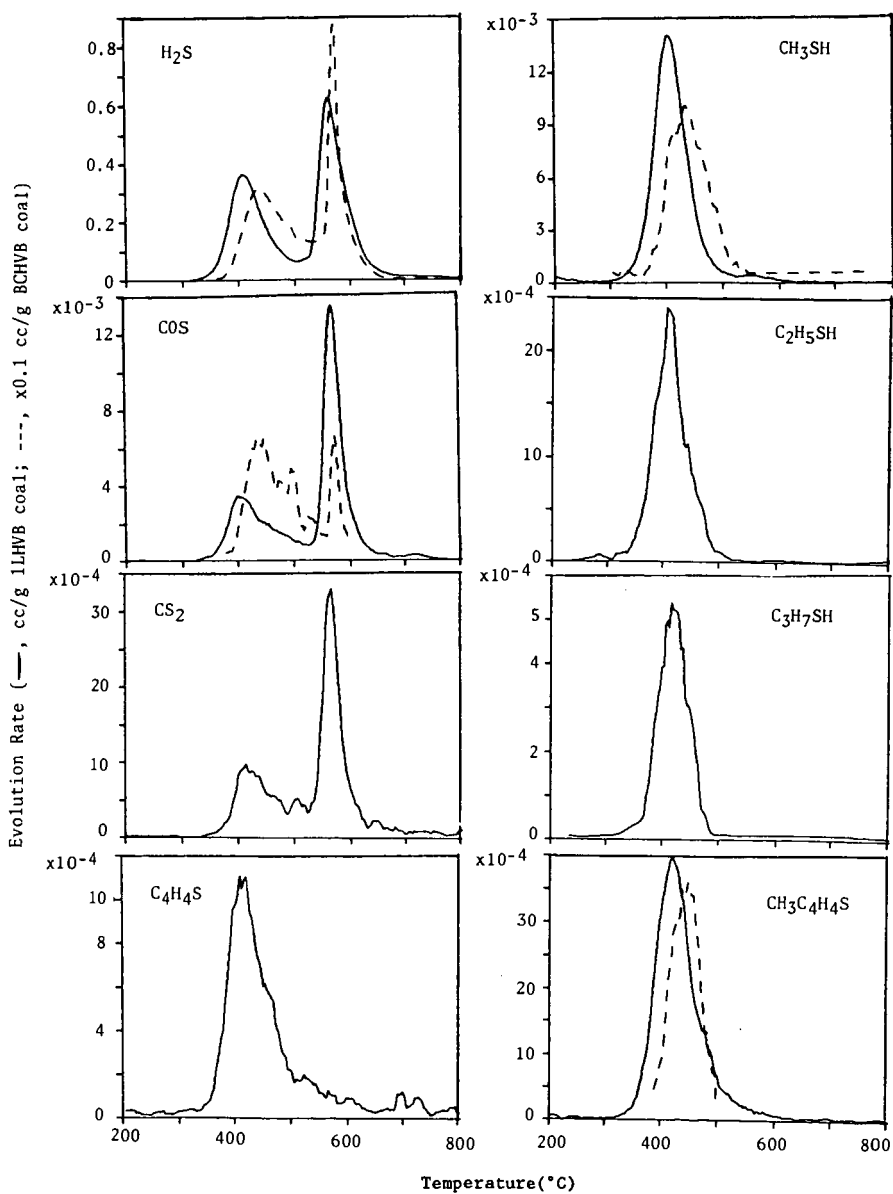


Fig. 2. Evolution profiles of eight sulfur gases.



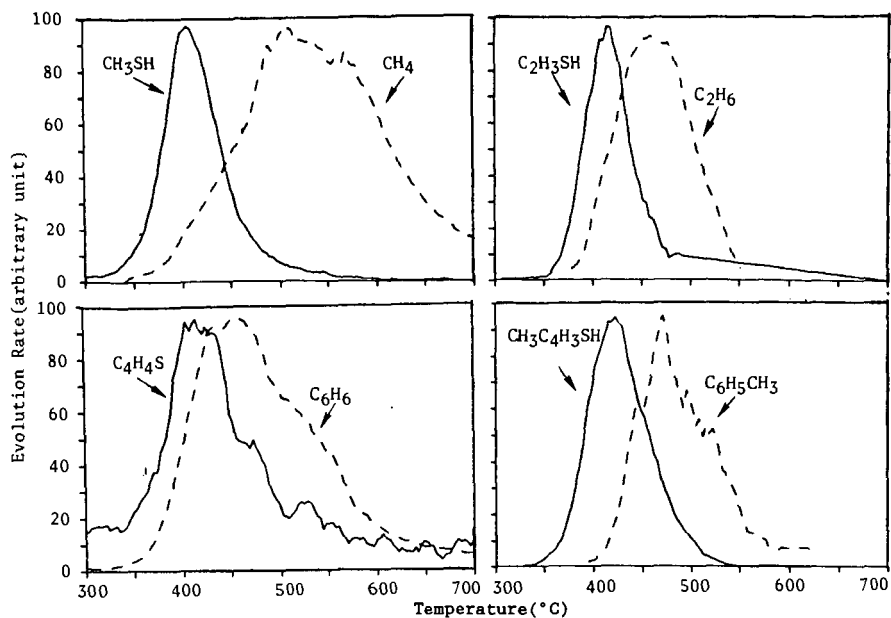


Fig. 3. Comparison of sulfur gas evolution with hydrocarbons.

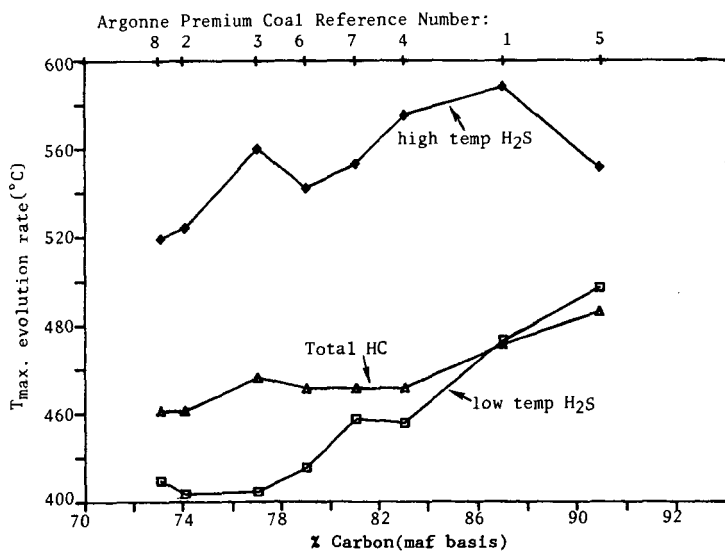


Fig. 4. Variation of  $T_{\text{max}}$  for  $\text{H}_2\text{S}$  and total hydrocarbon gases and naphtha (HC) with coal rank